ELSEVIER

Medical Engineering & Physics 25 (2003) 79–90

Medical Engineering & Physics

www.elsevier.com/locate/medengphy

Review

A review of electrical impedance techniques for breast cancer detection

Y. Zou *, Z. Guo

Department of Electrical and Computer Engineering, The George Washington University, 801 22nd Street NW, Washington, DC 20052, USA

Received 19 February 2002; received in revised form 14 September 2002; accepted 15 October 2002

Abstract

Some evidence has been found that malignant breast tumors have lower electrical impedance than surrounding normal tissues. Although the separation of malignant tumors from benign lesions based on impedance measurements needs further investigation, electrical impedance could be used as an indicator for breast cancer detection. In this paper, we provide a systematic technical review of the existing electrical impedance techniques proposed for breast cancer detection, with an emphasis on noninvasive impedance imaging techniques.

The electrical impedance of human breast tissue is first introduced, with tabulation of previous in vitro impedance measurement results on cancerous and normal breast tissues, and a brief description on the limited in vivo impedance measurements completed with invasive, or noninvasive, non-imaging techniques. A detailed review on noninvasive impedance imaging techniques for breast cancer detection, such as electrical impedance tomography (EIT) and electrical impedance mapping (EIM), is then presented.

We suggest that for better breast cancer detection, an invasive impedance technique may be enhanced by combination with other cancer indicators. 3D EIT should be improved through collective efforts. EIM using a pair of electrode arrays is a viable method with great potential. Magnetic induction tomography and other magnetic induction based impedance imaging for breast cancer detection are promising and merit further exploration as well.

Keywords: Electrical impedance; Breast cancer; Impedance imaging; Electrical impedance tomography; Impedance mapping

Contents

1. Introduction 80

2. Electrical impedance of human breast tissue 80
2.1. Electrical properties of human tissue 80
2.2. In vitro impedance measurements of human breast tissues 81
2.3. In vivo impedance measurements of human breast tissues 81

3. Noninvasive impedance imaging techniques 82
3.1. EIT 82
3.1.1. The work of Dartmouth College group 83
3.1.2. Electric impedance mammograph developed at Technical University of Gdañsk 84
3.1.3. TCI's electric mammograph 84
3.1.4. The proposed EIT system from Rensselaer Polytechnic Institute 85

* Corresponding author. Tel.: +1-202-994-0204; fax: +1-202-994-0227.

E-mail address: ynzou@seas.gwu.edu (Y. Zou).

1350-4533/03/$30.00
doi:10.1016/S1350-4533(02)00194-7

3.2. EIM technique 85
3.3. Magnetic induction tomography 87

4. Discussion and conclusion 87

1. Introduction

Breast cancer is the most common malignant tumor among women in the western world [1]. Early detection of breast cancer plays the leading role in reducing the mortality rate. Currently, X-ray mammography is the standard screening technique for breast cancer detection [2,3]. However, it has some limitations including reduced ability to detect carcinoma in women with dense breast tissue. In addition, due to the morphologic similarity between benign and malignant lesions, mammography is less useful as a diagnostic technique. Patients with positive mammographic findings require a biopsy for definitive diagnosis. Biopsies of breast lesions discovered in mammography screenings are negative for malignancy in up to 80% of patients [4]. Thus, while many early breast cancers are detected by mammography, many of the positive screening mammograms prove to be false positives. This means that screening based on X-ray mammography has rather low specificity, though it has high sensitivity. When undergoing breast biopsy, patients suffer from both physical and emotional trauma. A better pre-biopsy diagnostic technique would reduce the number of patients with benign breast lesions who undergo unnecessary diagnostic biopsy, and reduce patients' trauma and healthcare costs.

Other methods, such as ultrasound and magnetic resonance imaging (MRI) can aid in breast cancer diagnosis. However, these methods still have various limitations [5]. The current major uses of breast ultrasound are to differentiate cystic from non-cystic breast masses and guide breast biopsy [6,7]. Breast MRI is expensive and can only diagnose breast lesions in certain clinical situations. Nuclear medicine has also been proposed for breast cancer diagnosis but with limited success [5]. Today, neither mammography nor any other available imaging technology can distinguish breast cancer from benign breast lesions with certainty. X-ray mammography still remains the dominant modality for early breast cancer detection.

In the 1920s, Frick and Morse found significant difference of capacitance between malignant breast tumors and normal tissues [8]. Recently, using electrical impedance for breast cancer detection has emerged as a new field, since more evidence has been found that malignant breast tumors have significantly different impedivity than normal tissues [9–12]. Electrical impedance of tissue could thus be used as an indicator for breast cancer detection. New imaging techniques for breast cancer detection using electrical impedance have been proposed, as evidenced from the commercialization of TS2000 (an impedance-imaging device for breast cancer detection, Transcan Medical, Ltd., Migdal Ha'Emek, Israel; distributed by Siemens AG) [13]. It is our intention in this paper to conduct a systematic technical review on recent developments in this field to evaluate the existing techniques and find new opportunities to detect breast cancer using electrical impedance.

In the following sections, the electrical impedance of human breast tissue is first introduced, with tabulation of previous representative results of in vitro impedance measurements performed on cancerous and normal breast tissues, and a brief description on the limited in vivo impedance measurements completed with invasive, or noninvasive non-imaging techniques. Secondly, a detailed review on representative noninvasive impedance imaging techniques for breast cancer detection is presented. Discussion and conclusion are given thereafter.

2. Electrical impedance of human breast tissue

2.1. Electrical properties of human tissue

It is well known that the electrical properties of biological tissues differ significantly depending on their structures. Human tissue consists of an aggregation of cells surrounded by fluids. Each cell has a membrane enveloping intracellular fluid. The intracellular and extracellular fluids that contain water, electrolytes, etc., are basically resistive. The membrane constituted by a thin lipid bilayer with leaky ion-channels is both capacitive and resistive.

Since electrical impedance of human tissue contains both resistance and capacitance, it is complex and can be described by a serial representation

$$Z = R + jX$$

where, Z is impedance; R, the resistance; and X, the reactance; or by a parallel representation

$$Y = G + j\omega C$$

where, $Y = 1/Z$ is admittance; G, the conductance; C, the capacitance; and ω, the angular frequency. An alternative way to represent tissue admittance is by admittivity, expressed as

$$\sigma^* = \sigma + j\omega\varepsilon_0\varepsilon'$$

where, $\sigma^*$is tissue admittivity; σ, the tissue conductivity; ϵ', the tissue permittivity; and ϵ_0, the dielectric constant of free space.

The electrical properties of tissue vary with the frequency of the applied electric field as seen from α-, β- and γ-dispersion [14]. The α-dispersion occurs at low frequencies (10 Hz–10 kHz) and is mainly affected by the ionic environment that surrounds the cells. The β-dispersion is a structure relaxation in the frequency range 10 kHz–10 MHz. At higher frequencies, the γ-dispersion is found related to water molecules. The α- and β-dispersion regions are more interesting in medical applications, since most changes between pathological and normal tissue occur in this range [15]. The impedance of tissue also varies with temperature and time [16]. It is also anisotropic [16,17]. (The readers may refer to [18,19] for extensive reviews on tissue's electrical properties.)

2.2. In vitro impedance measurements of human breast tissues

Since the 1920s, various researchers have done in vitro impedance measurements on excised normal and cancerous human breast tissues. These basic researches have laid the ground for the continuing development of impedance-based techniques for breast cancer detection. Some representative results [8,9,20–25] were summarized in Table 1. From these in vitro impedance measurement results that are expressed in various terms, a common conclusion can be drawn that there are significant differences in electrical impedance between normal and malignant human breast tissues. Compared with surrounding normal tissues, malignant tumors showed typically higher conductivity [9,20], and/or permittivity [8,9,20,24], or lower impedivity [21,25]. The changed electrical properties of malignant tissue with respect to healthy tissue are attributed to increased cellular water and salt content, altered membrane permeability, changed packing density, and orientation of cells [27]. It is reasonable to conclude that malignant breast tumors have typically lower electrical impedance (impedivity) than surrounding normal tissues. Electrical impedance of tissue could thus be used as an indicator for breast cancer detection. Table 1 also suggests that the appropriate frequency range for impedance measurement for breast cancer detection should be 100 Hz–10 MHz, which is in the α- and β-dispersion regions. At higher frequencies in the β-dispersion region, permittivity shows more significant diagnosis value [24].

2.3. In vivo impedance measurements of human breast tissues

For breast cancer detection, the electrical impedance based techniques can be classified into two categories: invasive and noninvasive. In invasive techniques, needle electrodes are inserted into the tissue under study. A tiny ac current is applied to the tissue via a pair of current electrodes usually in a four-electrode configuration [28]. Voltage responses are measured using another pair of voltage electrodes. Noninvasive techniques include those of imaging type, as reviewed in the subsequent sections, and those of non-imaging type as introduced below. In any in vivo impedance measurement, the amplitude of the applied signal should be selected or controlled such that safety limits are never exceeded [29,30].

Morimoto et al. [11,31] performed in vivo invasive impedance measurement of breast tissue over the frequency range of 0–200 kHz using a three-electrode method (Fig. 1). In this method, two electrodes were embedded within a coaxial needle. The outer one was used for current input and the inner one for voltage output. A large reference electrode was placed on the abdomen of the subject. A pulse current with amplitude of 5 μA was applied. The measurement was done on 54 patients just before biopsy under general or local anesthesia. Using the measurement data, they calculated the parameters of an equivalent circuit consisting of a resistor R_e in parallel with a serial combination of a resistor R_i and a capacitor C_m. The results showed that R_e and R_i of malignant breast tumors were 'significantly higher than those of benign tumors ($p < 0.01$)'; C_m of breast cancer was 'significantly lower than that of benign tumors ($p < 0.01$)'. They suggested that impedance measurement might be used for the differential diagnosis of malignant and benign breast tumors. Compared with the results from the study [24] by Jossinet, the above results are not in agreement concerning C_m, though being consistent regarding R_e [24].

Using external electrodes and an impedance bridge in the frequency range of 100 Hz–100 kHz, Singh et al. [32] performed in vivo noninvasive impedance measurements on female breasts some of which contained tumors. Their results showed that malignant tumors have higher relative permittivity and lower resistance than those of normal breast tissue. Ohmine et al. [33] carried out noninvasive impedance measurements on 24 patients using a four-electrode technique. Their results suggest that differential diagnosis of breast tumors is possible by measuring the mammary electrical impedance using noninvasive electrodes on the skin.

From the above review on representative results of in vitro and in vivo impedance measurements on human breast tissues, it can be seen that malignant breast tumors have typically lower electrical impedance than surrounding normal tissues. Therefore electrical impedance may be used as an indicator for breast cancer detection. Studies [8,24,31,33] also demonstrated that there are significant differences in electrical impedance between benign and malignant breast tumors. Electrical impedance could thus be used to separate benign from malignant tumors

Table 1
Examples of in vitro impedance measurements of human breast tissues

Studies	Main results and comments
[8] 20 kHz	Studied 58 patients 'comprising all the cases of tumors of the breast'. The capacity of malignant tumors of the breast is 'consistently larger than that of normal tissues in the same location or of benign tumors'. The specific capacitance is from 107–583 pF for normal tissues and from 545–2860 pF for malignant tumors.
[20] 3 MHz–3 GHz	σ and ϵ of malignant tissues are higher than those of normal tissue, particularly at frequencies below 100 MHz. σ is from about 1.5–3 mS/cm for normal tissues and from 7.5–12 mS/cm for the malignant tissues. ϵ is about 10 for normal tissues and from about 50–400 for malignant tissues.
[21] 0.5 kHz–1 MHz	The modulus of impedivity of cancerous tissue (about 400 Ω cm at 1 kHz) is lower than that of non-pathologic fatty tissue (about 2000 Ω cm). The modulus of impedivity of the tissue at tumor center, half way from tumor center, and near the tumor, increases.
[9] 20 kHz–100 MHz	Comparison with tissues surrounding the tumor and peripheral tissue, cancerous tissue show higher σ and ϵ. Based on the data from 'a few typical tissue samples,' σ ranges from 0.3–0.4 mS/cm for normal tissue, from 2.0–8.0 mS/cm for 'central part of tumor'; ϵ ranges from 8–800 for normal tissue and from 80–above 10000 for 'central part of tumor'.
[22] 3.2 GHz	No significant difference in σ and ϵ of benign and malignant tumors. (It may be attributed to the overshadowing effect of polar water on the changes that may result from biologically different structures [26].)
[23] 5 kHz	Fitted data on three-component ($R1$–C–$R2$) model. $R1$ and $R2$ were higher, and C was lower in cancerous tissue than in normal tissue. Ulcerative growing carcinoma showed increase in C and decrease in $R1$ and $R2$.
[24] 0.488 kHz–1 MHz	The impedivity modulus for cancerous tissue (243 ± 77 to $383 \pm 97\Omega$cm) is lower than that of adipose subcutaneous fatty tissue (1747 ± 283 to $2188 \pm 338\Omega$cm) and connective tissue (859 ± 306 to $1109 \pm 371\Omega$cm), and higher than that of fibro-adenoma (200 ± 52 to $245 \pm 70\Omega$cm). No significant difference in impedivity between groups of normal tissue and benign pathology (mammary gland, matopathy and fibro-adenoma). At frequencies above 100 kHz, the cancerous tissue group has greater phase angle than any other group and 'exhibits the most capacitive response of all groups'.
[25] 1 kHz–10 MHz	Complex conductivity (i.e. admittivity) and characteristic frequency are largest for cancerous tissue, middle for transitory tissue and lowest for the healthy one.

and hence reduce the benign biopsies. However, the limited results on the electrical properties of benign and malignant breast tumors seem to be controversial. For example, some studies [8,24] demonstrated that malignant tumors have higher capacitance than benign tumors, while the study [31] showed that malignant tumors have lower C_m than benign tumors. This could be due to the employment of different measurement techniques, differences in in vitro and in vivo conditions of tissues, or variations of tissue samples. Further study is required to investigate the electrical impedance of benign and malignant tumors for better differential diagnosis of breast cancer.

Instruments for invasive impedance measurement can have low cost and fast response. They may be combined with needle biopsies to aid the localization of malignant tumors [31] to increase the diagnosis accuracy. However, due to their invasive nature, extra care should be taken to further investigate their appropriateness for routine clinical use in breast cancer detection. As for less complex noninvasive non-imaging techniques, such as the one used in Ref. [33], their effectiveness in breast cancer detection is yet to be seen. So far, some noninvasive impedance imaging-based techniques have been proposed for breast cancer detection, as described later.

3. Noninvasive impedance imaging techniques

3.1. EIT

Noninvasive impedance imaging techniques may be classified into two main categories: electrical impedance tomography (EIT) and electrical impedance mapping (EIM). (For more detailed references on EIT, the readers may refer to Refs. [28,34,35]. Here we only provide a basic introduction on EIT.)

In EIT, a large number of impedance measurements are made from electrodes placed on the body surface and the results are processed by a computer to produce

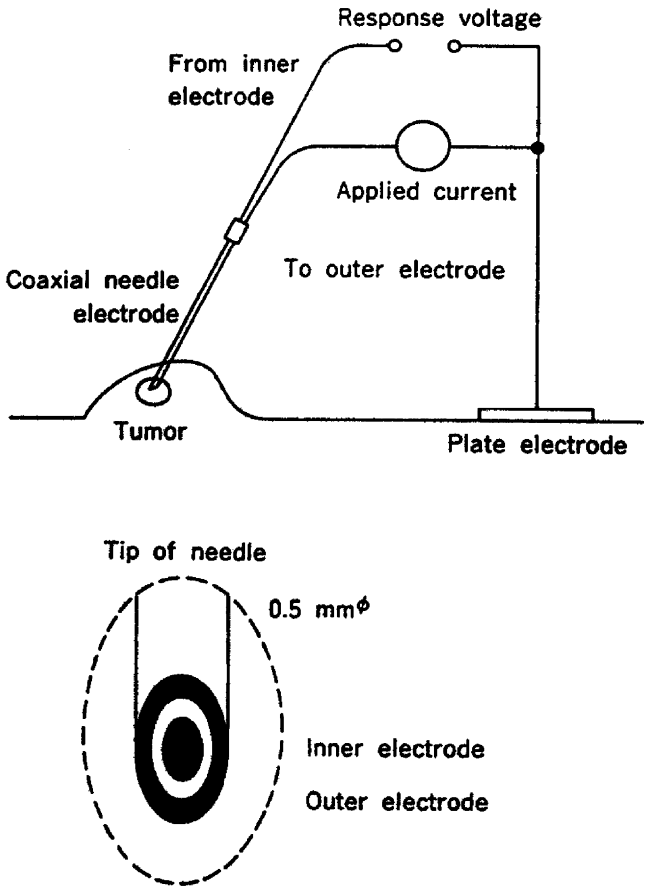

Fig. 1. In vivo impedance measurement using a three-electrode method. (Copyright ©1993. From Ref. [11]. Reproduced by permission of Taylor & Francis, Inc., http://www.routledge-ny.com).

reconstructed tomographic 2D or 3D images of the impedance (conductivity and/or permittivity) distribution within the body. EIT imaging is based on the significant electrical impedance variation between different tissue types [34]. Both static and dynamic imaging exists in EIT. The static imaging involves producing an image of the distribution of absolute conductivity or impedivity, while the dynamic imaging reconstructs images of change in conductivity, derived from a change in the electrode voltages [34]. The success of an EIT system relies on its data acquisition and image reconstruction.

On the data acquisition, most practical EIT systems operate on a so called 'current-driving mode', namely, applying a known, constant ac current to two or more electrodes, and measuring the voltages developed between other electrodes [34]. Conversely, the 'voltage-driving mode' is defined as applying a known ac voltage to two or more electrodes and measuring the currents through other electrodes. Various data acquisition techniques have been proposed. They mainly differ in the number and arrangement of electrodes, the excitation mode (i.e. current or voltage driving mode), the pattern of the excitation signal, and the working frequency range. Though being conceptually simple, the data acquisition process in EIT imaging is difficult to implement in practice [34].

The image reconstruction of EIT is a challenging inverse problem, which is both nonlinear and ill posed [35]. It involves solving a forward problem defined as given a known impedance distribution, calculate the measured surface voltages from the applied currents, and an inverse problem defined as given the measured surface voltages, calculate the unknown impedance distribution. Current reconstruction algorithms are often based on finite element modeling, with Poisson's equation being the governing equation and the assumption of a quasistatic condition, since the working frequencies in EIT are relatively low ($<$1 MHz). The various proposed EIT image reconstruction algorithms may be classified as single-step (non-iterative) type or iterative type [34]. The reconstruction techniques of single-step type include back-projection [36] and sensitivity matrix methods [37]. The variants of Newton–Raphson method [38] are the most popular iterative reconstruction technique [34].

EIT has been extensively investigated by over 20 groups for its clinical applications mainly in studying gastric function, pulmonary ventilation, perfusion, and hyperthermia [34]. EIT for breast cancer detection has also been actively studied by a limited number of research groups. The representative works are reviewed as follows.

3.1.1. The work of Dartmouth College group

Hartov et al. [39] built and tested a 32-channel, multi-frequency (DC to 1 MHz) 2D EIT system. The resolution of the A/D converter was 16-bit with a 200 kHz sampling frequency [40]. Ag/AgCl electrodes were used in the system. The system simultaneously applied a voltage signal and measured currents at all electrodes. Magnitudes and phases of impedance were calculated using the reference voltage and the response current signals. Image reconstruction was based on the Newton method [41]. In their finite element modeling, they used a dual mesh approach: a fine mesh for voltage calculation in the forward problem; a coarse mesh for calculating conductivity and permittivity in the inverse problem [40]. This system was evaluated by Kernnel et al. [42] using an EIT phantom.

Osterman et al. [43] modified the EIT system to investigate its feasibility for routine breast examinations. In their in vivo test, 16 electrodes formed an electrode array and were in direct contact with the breast through a 'radially translating interface' as shown in Fig. 2(a). The electrode array was located below an examination table, on which a participant would lie prone with the breast to be imaged pendant in the array. Ac voltage signals were delivered to the electrodes over the 10 kHz–1 MHz frequency range. Multi-channel measurements were conducted at 10 frequencies on both breasts. Thirteen

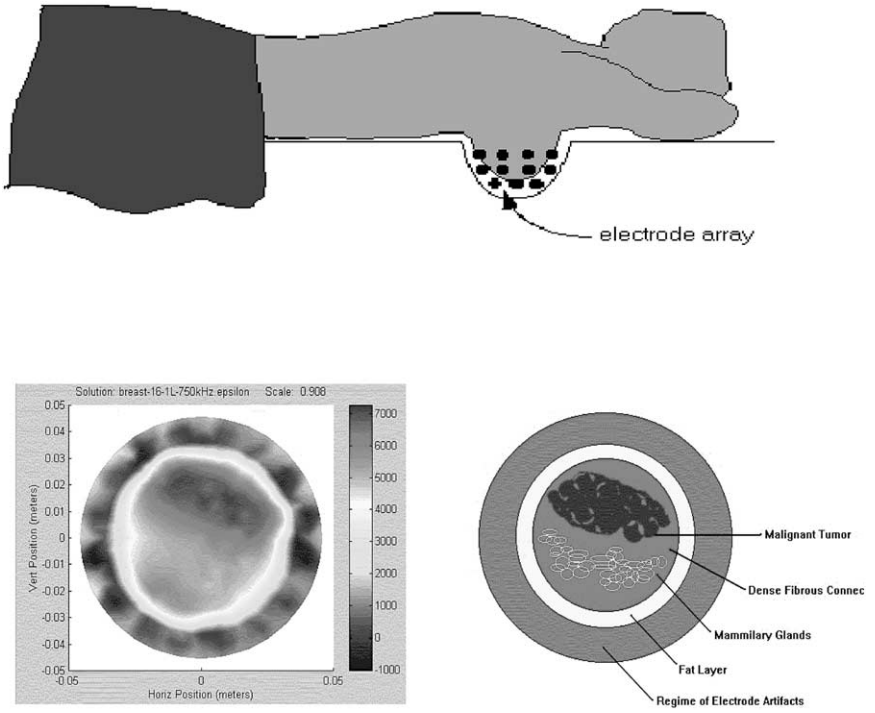

Fig. 2. The EIT system of Dartmouth College: (a) electrode setup; (b) absolute permittivity image (coronal view of breast with malignant tumor at 750 kHz). (From http://www-nml.dartmouth.edu/biomedprg/EIS/index.html. By permission.)

women were tested. The examination of each breast took about 10 min. The results showed that structural features in the EIT images correlated with limited clinical information available on participants. However, near-surface electrode artifacts were evident in the reconstructed images (Fig. 2(b)). They concluded that their system was sensitive, but not very specific—good for ruling out tumors [40]. An initial study on the consistency of the exam has been performed with an improved breast interface [44]. With increasing levels of electrode placement uncertainty, they imaged 25 breasts in four separate 'substudies'. Their results suggest that their EIT breast exams are 'consistent provided the electrode placement is well controlled, typically with better than 1 cm accuracy'. The major limitation of Dartmouth's EIT system is its 2D impedance measurement nature, although the system has both vertical and radial electrode array positioning capability.

3.1.2. Electric impedance mammograph developed at Technical University of Gdañsk

Wtorek et al. [45] built an experimental 3D EIT system for breast cancer detection. It includes a sensing head, a digital signal processor, and a personal computer. The sensing head contains a hemisphere chamber of 16-cm diameter with 64 annular compound electrodes placed at fixed multi-layer positions. Current or voltage is applied through the outer electrode and the inner one measures response voltage or current, respectively. In its current-driving mode, the device measures the potential difference between various pairs of electrodes. The measured potential differences are sent to the computer to reconstruct and display 3D impedance distributions in the hemisphere. The image reconstruction is based on the perturbation method [41]. The configuration of this system could have some distinct advantages. As pointed out by Wtorek et al. [45], the fixed geometry of the chamber could minimize any problems introduced by uncertainty of the object geometry. Moreover, introducing saline solution between the examined object and the surface electrodes would stabilize the contact impedance during in vivo measurement. One limitation of this system is that only 64 electrodes are used, insufficient for obtaining satisfactory resolution in 3D. Also the arrangement of electrodes on a fixed hemisphere might limit the application of this device, since the contact between skin and electrode may only be provided for a breast of definite size [46].

3.1.3. TCI's electric mammograph

Cherepenin et al. [46,47] described an innovative electric mammograph patented by TCI (Technology Commercialization International Inc., Albuquerque, NM, USA). It is a 3D EIT system as shown in Fig. 3(a). A compact array of cylindrical protruding electrodes made of stainless steel is arranged in a rigid dielectric plane. (In Fig. 3(a), 256 electrodes were used.) Two additional singular electrodes are used as ac current source and potential reference, respectively. Each can be located on a wrist, as shown in Fig. 3(b). During the examination,

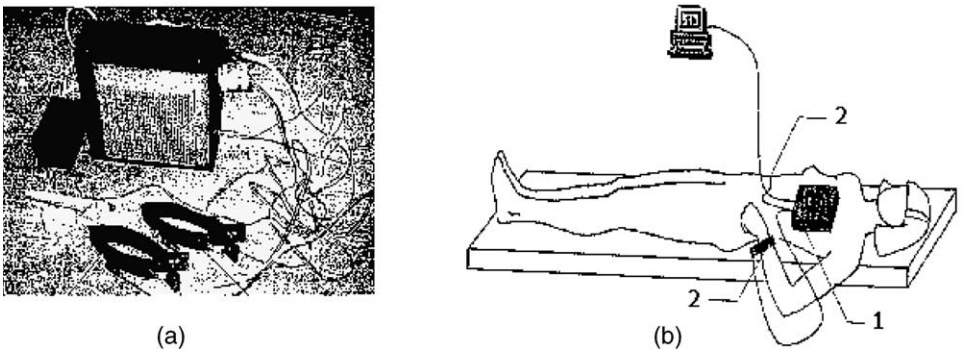

Fig. 3. TCI's electric mammograph: (a) the sensor plates and the reference electrodes; (b) the use and configuration of the device: 1—plane with 256 electrodes, 2— remote electrodes [36]. Reproduced by permission of Technology Commercialization Incorporated, NM, USA.)

the electrode plane is pressed against the breast, flattening it toward the chest. A 10 kHz ac current source, about 1 mA, is connected between the remotely attached current electrode and one of the electrodes in the planar array. The potential difference between the selected atrest electrode in the planar array and the remote reference electrode is measured. For each input electrode, the output multiplexer sequences through all the other electrodes in the array while the potential difference is measured. The input electrode is switched and the output multiplexer sequence repeated, resulting in 65 280 (256×255) voltage measurements for each full measurement cycle [47]. Images for 3D conductivity distribution are reconstructed using a modified back projection method [46].

Features of this system include that pressing the plane against the breast can increase the number of electrodes in contact with the breast and also reduce the thickness of tissue layers to be measured. Due to the long distances between the singular electrodes and the electrode plane, it may be assumed that the unperturbed equipotential surfaces of the electrical field be spherical in the examination area, which simplifies image reconstruction [46]. Another feature of this device lies in the threshold detector of output voltages to identify those electrodes that have insufficient electrode-body contact. During the reconstruction, the potential difference values coming from insufficient-contact electrodes are replaced by values calculated on the assumption of a homogeneous conductivity distribution [46]. Cherepenin et al. [47] reported the results of its preliminary clinical trial on 21 women. Eighty-six percent of examinations were found to fully or partially agree with diagnoses made by X-ray mammography and biopsy.

3.1.4. The proposed EIT system from Rensselaer Polytechnic Institute

The EIT research group in Rensselaer Polytechnic Institute (RPI) is also interested in using impedance imaging for breast cancer detection [48,49]. Mueller et al. [49] studied the use of a rectangular electrode array mounted on the surface of a region to collect voltage data and create 3D impedance images for the subspace under the electrode array. They expected this electrode configuration might be desirable for detecting human breast tumors using EIT. They performed numerical simulation and phantom studies for a 4×4 electrode array. In their phantom study, each copper electrode measured 5×7mm. A saline filled rectangular tank was used in which electrode-sized agar targets ($5 \times 7 \times 5.5$mm) were suspended at several positions. The saline solution's conductivity (300 mS/m) was chosen to approximate that of healthy tissue and the conductivity of the agar (900 mS/m) was chosen to approximate that of a malignant tumor. They applied normalized eigenfunction current patterns [50] on the 16 electrodes. The subspace under the electrode array was discretized into $4 \times 4 \times 4$ voxels. Their reconstruction algorithm was based on linearizing the conductivity about a constant value. Their experiment results showed that in the plane of the electrodes the inhomogeneity's position is well characterized in the reconstruction, but with poor depth resolution. As suggested by Mueller et al. [49], it is possible to improve this method by using more electrodes in the array, better modeling of the shunting and surface impedance effects of the electrodes, and applying an improved reconstruction algorithm. So far, no practical EIT system for breast cancer detection has been developed from RPI.

3.2. EIM technique

In EIM, constant ac voltage is applied to the body usually between an array of multiple sensing electrodes covering the surface of the body to be imaged, and a large reference electrode placed elsewhere on the body. The multiple sensing electrodes are kept at an equal potential while the currents through the electrodes are measured. The calculated values of the local bulk impedance underneath the sensing electrodes are then projected to the surface and mapped as 2D images. Being

conceptually more straightforward than EIT, EIM requires literally no complex image reconstruction.

Using EIM, TS2000 is so far the only commercially available electrical impedance-imaging device for breast cancer detection. TS2000 includes a reference electrode held in a patient's hand, and a scan probe, pressed against the breast [27] as shown in Fig. 4. The reference electrode is a metallic cylinder (diameter 3.4 cm, length 12 cm) and the scan probe contains a planar array of rectangular electrodes (16×16 on the large and 8×8 on the small probe) separated by rectangular grids. Each electrode has an area of 3×3mm. The center-to-center distance between electrodes is 4 mm, leaving 1 mm of space between adjacent electrodes. A guarding ring in the form of 7-mm wide metallic strip surrounds the sensing area to hinder the electrical edge effects. Conductive gel is used as medium between the sensing area and the breast surface.

During the measurement using TS2000, an ac voltage of 1–2.5 V is applied between the handheld reference electrode and the measuring electrodes on the probe kept at virtual ground [51]. The current travels from the patient's arm to the highly conducting pectoralis muscle, which may be considered as an isopotential plane. Therefore, a roughly parallel electric configuration is created between the pectoralis muscle and the probe pressed on the breast of the supine patient. Based on this configuration, pressing the probe on the breast by the physician during examination will decrease the distance between the measuring probe and the pectoralis muscle, hence increasing the sensitivity for detecting the distorted electric field due to the existence of a malignant tumor. Within the measurement frequency range of 50 Hz–20 kHz [13], the amplitude and phase of the induced current on each measuring electrode are calculated. The source signal is also sampled and serves as a reference signal. These signals coupled with the system's transfer function are used to compute the admittance at each electrode. Conductance and capacitance related maps are displayed in gray levels on the monitor.

Since cancerous tumors have relatively high conductivity and permittivity with respect to surrounding healthy tissues, a cancerous tumor causes enhanced current signals measured by the electrodes close to the lesion. In TS2000's gray-level images, the cancer is thus visualized as a focal white spot [27]. Multiple clinical studies on using TS2000 for breast cancer detection have been conducted. In a clinical study performed on a total of 504 biopsied breasts consisting of 179 malignant and 325 benign findings, three methods—T-scan alone, mammogram, adjunctive T-scan i.e. combination of T-scan and mammogram, were used. The results show that, as an adjunct to X-ray mammography, T-scan improved mammographic specificity from 39–51% ($p = 0.0003$) and increased mammographic sensitivity of 82–88% ($p = 0.01$). The results for the 273 mammographically equivocal cases show that, with adjunctive T-scan reading, mammographic specificity was increased significantly from 60–82% ($p = 0.02$) and mammographic sensitivity was also increased significantly from 41–57% ($p = 0.0003$) [13]. Due to the promising clinical trial results, TS2000 was granted US FDA's pre-market approval in 1999 for adjunctive use with X-ray mammography [13]. It has been shown that this device provides additional information for guiding a biopsy recommendation.

Although TS2000 is the only commercially available impedance-imaging device for breast cancer diagnosis, a number of limitations have been found from clinical studies. The major limitations can be summarized as follows [52]:

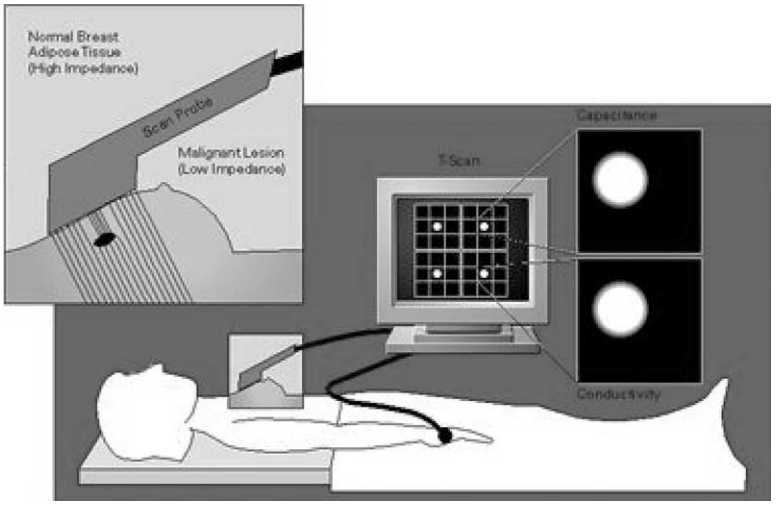

Fig. 4. The system configuration and basic principle of TS2000. A constant voltage is applied between the handheld electrode and the rectangular electrode array in the probe. A malignant lesion causes enhanced current density that can be detected by the probe. The lesion is shown as a focal bright spot on the conductance and capacitance maps. (From http://www.med.siemens.com/medroot/en/prod/diag/womens/prod/trans/prin/imaging/index.html. Reproduced by permission of Siemens AG.)

1. false positives caused by artifacts such as air bubbles, interfering bones, muscles, and superficial skin lesions, resulting in high conductivity measurement, or bright spots;
2. limited maximum depth of measurement is 3–3.5 cm, hindering detection of lesions close to the chest wall;
3. not possible to localize positive lesion for biopsy.

3.3. Magnetic induction tomography

Magnetic induction tomography (MIT) can also be used for impedance imaging. Unlike EIT or EIM, MIT does not require electrical contacts with the body; instead it uses the interaction of an oscillating magnetic field with conductive media. The field, perturbed by eddy currents in the object, can be excited and measured by small coils arranged around the object. The conductivity (and permittivity) can be reconstructed from the measurements of the perturbed magnetic field outside the object. Earlier work in MIT was performed by Gençer et al. [53–56]. Recently, Griffiths et al. [57] developed an MIT system for measuring biological tissue. Korjenevsky et al. [58] also developed an MIT system. Scharfetter et al. [59] studied sensitivity maps of MIT. Their work demonstrated the applicability of MIT for medical imaging and diagnostics. Being a potential technique, however, to the authors' knowledge, MIT and other magnetic induction based impedance methods have not been studied for breast cancer detection.

4. Discussion and conclusion

Electrical impedance has been used for tackling a challenging problem—the detection of breast cancer for over 70 years. Intensive in vitro and limited in vivo measurements support the efforts in further developing impedance-based invasive or noninvasive techniques for breast cancer detection. Invasive impedance techniques could have advantages of low cost and fast response. However, the accuracy of tumor localization and the design of electrodes need to be improved before invasive methods could be used in clinical settings. Their detection accuracy may also be improved from combinational use with other cancer indicators, as evidenced by the development of 'smart needle' from BioLuminate, Inc., San Jose, CA. By combining impedance measurement with measurements of oxygen partial pressure, temperature, light scattering and absorption properties including deoxygenated hemoglobin, vascularization, and tissue density, the smart needle technique has the potential to achieve high detection accuracy [60].

Within the noninvasive imaging based techniques, EIT is an active candidate and its hardware and image reconstruction algorithms have been studied for about 20 years. However, a series of problems still exist that limit its clinical applications, including breast cancer detection. The key limitation is their low spatial resolution. The main reasons include inaccurate modeling of the system, varying electrode–skin contact impedance, limited number of independent measurements, and poor signal to noise ratio [61–68]. Kolehmainen et al. [67] pointed out the parameters that most affect the reconstructed image are the contact impedance under the electrodes, sizes and locations of the electrodes, and the boundary shape of the object. They suggested that the most feasible way to minimize these errors is to measure them and to utilize the data in the forward modeling.

Due to the limited number of electrodes used in current EIT systems, increasing the number of electrodes seems to be a viable solution to increase the number of independent measurements, hence possibly improving the spatial resolution. However, simply increasing the number of electrodes will not only add to the complexity of the hardware and software, but also increase the need to deal with problems associated with electrode positioning and localization. In a limited space, such as a human breast, the number of applicable electrodes is limited, since a current electrode should have sufficient size to reduce the current density under the skin [64]. Also, the interconnections, such as cables from electrodes to the successive circuitry, need space as well. Although various electrode systems for EIT have been used as reviewed by McAdams et al. [69], applying a large amount of electrodes to the breast with high reliability and good contact remains a difficult problem. Jossinet [70] proposed a pneumatic activated electrode system to facilitate automatic electrode attachment to the breast. Holder [71] designed a conical array for breast imaging, which comprised five electrode rings with differing diameter to fit to any breast size. The device provided good electrode–skin contact by application of vacuum, depression and rotation of the specially designed electrodes. Nevertheless, these attachment approaches do not help greatly with spatial resolution, because the number of independent measurements was not increased. A possible solution to the electrode–skin contact problem is suggested by Wtorek et al. [45], that is to fix the electrodes on a rigid surface and enable their contact with breast through a conductive media such as saline with appropriate conductivity. Cornish et al. [72] suggested optimizing electrode site might also help improve impedance measurements. Concisely, to truly improve the spatial resolution of an EIT system, reliable electrode attachment and increasing the number of independent measurements must be considered together.

For breast cancer detection, ideally 3D images could be formed based on EIT so that not only a tumor's benign or malignant status but also its location could be indicated accurately. Using 3D EIT may not only improve tumor localization to aid biopsy, but also help to filter out false positive results caused by artifacts such

as skin lesions, bones, etc. However, this requires an EIT system having sufficiently high spatial resolution and high reproducibility. To achieve this, collective efforts should be made, including increasing the number of independent measurements and using reliable electrode–skin contact means, attempting different data collection schemes, and deriving novel reconstruction algorithms. The multi-frequency approach may further increase the detection accuracy [27]. The EIT system in [46] is a good example that can generate 3D images by utilizing a special signal injection pattern, substantially increasing the number of electrodes, and measuring and correcting for bad electrode–skin contacts.

As for EIM, the limitations of TS2000 can give us good insights on how to improve the technique for better breast cancer detection. An improved impedance-mapping technique may utilize a pair of electrode arrays, one for exciting and one for measuring. During the examination, the breast would be compressed between the electrode arrays, and impedance images of both mediolateral oblique and craniocaudal views could be generated, similar to conventional X-ray mammography. Since the impedance images could be compared directly with X-ray mammograms, this technique may increase the accuracy of breast cancer detection and may also aid in biopsy localization. Our group is currently investigating this technique.

MIT or magnetic induction-based impedance imaging has the potential for breast cancer detection. A stronger eddy current may be induced in a malignant tumor and its associated magnetic field may be detected from external measurement. The major advantage of these kinds of methods is that they can avoid the problems related to electrode–skin contact. Smith et al. [73] tried a similar method for prostate cancer study. Their results are promising. However, if magnetic induced impedance imaging is used for breast cancer detection, the difficulty could be the detection of the very weak signals that come from a small sized tumor close to the chest. This might be mitigated by pressing the breast toward the chest, or compressing the breast between two plates.

Combining electrical impedance measurement with other modalities, such as mammography, ultrasonography and thermography, can open up new opportunities for breast cancer detection. For example, based on the pilot study by Jossinet et al. [74], an integrated breast-scanning probe that combines both ultrasound and electrical impedance measurement could be invented in the future.

It is worth noting that current evidence supporting the separation of benign from malignant breast tumors using electrical impedance techniques is very limited. Further studies on this issue are necessary to fully utilize electrical impedance based techniques for breast cancer detection, especially for the differential diagnosis of breast cancer. If this is successful, the reduction of benign biopsies could be expected.

From this focused review on electrical impedance techniques for breast cancer detection, we are able to find various opportunities for improving current EIT and mapping-based methods, and for future development of new techniques, such as MIT for breast cancer detection. We suggest that 3D EIT should be improved through collective efforts. Impedance mapping using a pair of electrode arrays is a viable method and has great potential. MIT and other magnetic induction based impedance imaging for breast cancer detection are promising and merit further exploration as well.

Acknowledgements

This work was partially supported by Susan G. Komen Breast Cancer Foundation through a breast imaging research grant.

References

[1] Boring CC, Squires TS, Tong T. Cancer statistics. CA Cancer J Clin 1994;44:7–26.
[2] Simonetti G, Cossu E, Montanaro M, Caschili C, Giuliani V. What's new in mammography. Eur J Radiol 1998;27:S234–S41.
[3] Elmore J, Barton M, Moceri V, Polk S, Arena PJ, Fletcher SW. Ten-year risk of false positive screening mammography and clinical breast examinations. New Engl J Med 1998;338:1089–96.
[4] Burns RP. Image guided breast biopsy. Am J Surg 1997;73:9–11.
[5] Edell SL, Eisen MD. Current imaging modalities for the diagnosis of breast cancer. Del Med J 1999;71:377–82.
[6] Bird RE, Wallac TW, Yankaskas BC. Analysis of cancer missed in the screening mammography. Radiology 1992;34:149–52.
[7] Stavros AT, Thickman D, Rapp CL, Dennis MA, Parker SH, Sisney GA. Solid breast nodules: use of sonography to distinguish between benign and malignant lesions. Radiology 1995;196:123–34.
[8] Fricke H, Morse S. The electrical capacity of tumors of the breast. J Cancer Res 1926;10:340–76.
[9] Surowiec AJ, Stuchly SS, Barr JB, Swarup A. Dielectric properties of breast carcinoma and the surrounding tissues. IEEE Trans Biomed Eng 1988;35:257–63.
[10] Schwan HP. Mechanisms responsible for electrical properties of tissue and cell suspensions. Med Prog Technol 1993;19:163–5.
[11] Morimoto T, Kimura S, Konishi Y, Komaki K, Uyama T, Monden Y et al. A study of the electrical bioimpedance of tumors. J Invest Surg 1993;6:25–32.
[12] Jossinet J. The impedivity of freshly excised human breast tissue. Physiol Meas 1998;19:61–75.
[13] FDA. 1999. Available from: http://www.fda.gov/cdrh/pdf/p970033.html.
[14] Pethig R. Dielectric properties of body tissues. Clin Phys Physiol Meas 1987;8:A5–A12.
[15] Blad B, Baldetorp B. Impedance spectra of tumor tissue in comparison with normal tissue: a possible clinical application for electrical impedance tomography. Physiol Meas 1996;17:A105–A15.
[16] Rabbat A. Tissue resistivity. In: Webster JG, editor. Electrical

impedance tomography. Bristol and New York: IOP Publishing; 1990. p. 8–20.
[17] Schwan HP. The practical success of impedance techniques from an historical perspective. Ann N Y Acad Sci 1999;873:1–12.
[18] Foster KR, Schwan HP. Dielectric properties of tissue and biological materials: a critical review. Crit Rev Biomed Eng 1989;17(1):25–104.
[19] Pethig R. Dielectric properties of biological materials: biophysical and medical applications. IEEE Transac Elec Insul 1984;EI-19(5):453–73.
[20] Chaudhary SS, Mishra RK, Swarup A, Thomas JM. Dielectric properties of normal & malignant human breast tissues at radiowave & microwave frequencies. Indian J Biochem Biophys 1984;21:76–9.
[21] Jossinet J, Lobel A, Michoudet C, Schmitt M. Quantitative technique for bio-electrical spectroscopy. J Biomed Eng 1985;7:289–94.
[22] Campbell AM, Land DV. Dielectric properties of female breast tissue measured in vitro at 3.2 GHz. Phys Med Biol 1992;37:193–210.
[23] Heinitz J, Minet O. Dielectric properties of female breast tumors. Proceedings of Ninth International Conference on Electrical Bio-Impedance. Heidelberg: University of Heidelberg; 1995. p. 356–9.
[24] Jossinet J. Variability of impedivity in normal and pathological breast tissue. Med Biol Eng Comput 1996;34:346–50.
[25] Stelter J, Wtorek J, Nowakowski A, Kopacz A, Jastrzembski T. Complex permittivity of breast tumor tissue. Proceedings of 10th International Conference on Electrical Bio-Impedance, Barcelona; 1998. p. 59–62.
[26] Rigaud B, Morucci JP, Chauveau N. Bioelectrical impedance techniques in medicine. Part I: Bioimpedance measurement. Second section: impedance spectrometry. Crit Rev Biomed Eng 1996;24(4-6):257–351.
[27] Scholz B, Anderson R. On electrical impedance scanning—principles and simulations. Electromedica 2000;68:35–44.
[28] Webster JG. Electrodes. In: Webster JG, editor. Electrical impedance tomography. Bristol and New York: IOP Publishing; 1990. p. 21–8.
[29] AAMI. American national standard: safe current limits for electromedical apparatus. Document ANSI/AAMI ES1—1993. 1993.
[30] IEC. International standard: medical electrical equipment—Part 1–2: general requirements for safety. Document IEC 60601-1-2. 2nd ed. (2001-09). 2001.
[31] Morimoto T, Kinouchi Y, Iritani T, Kimura S, Konishi Y, Mitsuyama N et al. Measurement of the electrical bio-impedance of breast tumors. Eur Surg Res 1990;22:86–92.
[32] Singh B, Smith CW, Hughes R. In vivo dielectric spectrometer. Med Biol Eng Comput 1979;17:45–60.
[33] Ohmine Y, Morimoto T, Kinouchi Y, Iritani T, Takeuchi M, Monden Y. Noninvasive measurement of the electrical bioimpedance of breast tumors. Anticancer Res 2000;20(3B):1941–6.
[34] Boone K, Barber D, Brown B. Imaging with electricity: report of the European concerted action on impedance tomography. J Med Eng Technol 1997;21(6):201–32.
[35] Cheney M, Isaacson D, Newell JC. Electrical impedance tomography. SIAM Rev 1999;41(1):85–101.
[36] Barber DC, Brown BH. Applied potential tomography. J Phys E Sci Instrum 1984;17:723–33.
[37] Zadehkoochak M, Blott BH, Hames TK, George RE. Special expansion in electrical impedance tomography. J Phys D Appl Phys 1991;24:1911–6.
[38] Yorkey TJ, Webster JG, Tompkins WJ. Comparing reconstruction algorithms for electrical impedance tomography. IEEE Trans Biomed Eng 1987;34:843–52.
[39] Hartov A, Mazzarese RM, Kerner TE, Osterman KS, Reiss FR, Williams D et al. A multi-channel continuously-selectable multi-frequency electrical impedance spectroscopy measurement system. IEEE Trans Biomed Eng 2000;47:49–58.
[40] Dartmouth College. 2001. Available from: http://www-nml.dartmouth.edu/biomedprg/EIS/index.html.
[41] Hua P, Woo EJ. Reconstruction algorithms. In: Webster JG, editor. Electrical impedance tomography. Bristol and New York: IOP Publishing; 1990. p. 97–137.
[42] Kerner TE, Williams DB, Osterman KS, Reiss FR, Hartov A, Paulsen KD. Electrical impedance imaging at multiple frequencies in phantoms. Physiol Meas 2000;21:67–77.
[43] Osterman KS, Kerner TE, Williams DB, Hartov A, Poplack SP, Paulsen KD. Multifrequency electrical impedance imaging: preliminary in vivo experience in breast. Physiol Meas 2000;21:99–109.
[44] Kerner TE, Hartov A, Soho SK, Poplack SP, Paulsen KD. Imaging the breast with EIS: an initial study of exam consistency. Physiol Meas 2002;23(1):221–36.
[45] Wtorek J, Stelter J, Nowakowski A. Impedance mammography 3D phantom studies. Ann N Y Acad Sci 1999;873:520–33.
[46] Cherepenin VA, Korjenevsky AV. Electric mammograph. WO patent WO053090A1. 2000.
[47] Cherepenin V, Karpov A, Korjenevsky A, Kornienko V, Mazaletskaya A, Mazourov D et al. A 3D electrical impedance tomography (EIT) system for breast cancer detection. Physiol Meas 2001;22:9–18.
[48] Larson-Wiseman J. Early breast cancer detection utilizing clustered electrode arrays in impedance imaging. PhD thesis. Troy, NY: Rensselaer Polytechnic. Institute; 1998.
[49] Mueller JL, Isaacson D, Newell JC. A reconstruction algorithm for electrical impedance tomography data collected on rectangular electrode array. IEEE Trans Biomed Eng 1999;46:1379–86.
[50] Isaacson D. Distinguishability of conductivities by electrical current computed tomography. IEEE Trans Med Imag 1986;5:92–5.
[51] Assenheimer M, Laver-Moskovitz O, Malonek D, Manor D, Nahaliel U, Nitzan R et al. The T-scan technology: electrical impedance as a diagnostic tool for breast cancer detection. Physiol Meas 2001;22:1–8.
[52] Malich A, Fritsch T, Anderson R, Boehm T, Freesmeyer MG, Freck M et al. Electrical impedance scanning for classifying suspicious breast lesions: first results. Eur Radiol 2000;10:1555–61.
[53] Gençer NG, İder TZ, Nakiboglu B. An alternative solution for the problem of electrode position determination in electrical impedance tomography. Annual International Conference of the IEEE Engineering. Med Biol Soc 1990;12:78–9.
[54] Gençer NG, İder YZ, Kuzuoglu M. Electrical impedance tomography using induced and injected current. Clin Phys Physiol Meas 1992;13:A95–A9.
[55] Gençer NG, İder YZ. A comparative study of several exciting magnetic fields for induced current EIT. Physiol Meas 1994;15:A51–A7.
[56] Gençer NG, İder YZ, Williamson SJ. Electrical impedance tomography: induced current imaging achieved with a multiple coil system. IEEE Trans Biomed Eng 1996;43:139–49.
[57] Griffiths H, Stewart WR, Gough W. Magnetic induction tomography. A measuring system for biological tissues. Ann N Y Acad Sci 1999;873:335–45.
[58] Korjenevsky A, Cherepenin V, Sapetsky S. Magnetic induction tomography: experimental realization. Physiol Meas 2000;21:89–94.
[59] Scharfetter H, Riu P, Populo M, Rosell J. Sensitivity maps for low-contrast perturbations within conducting background in magnetic induction tomography. Physiol Meas 2002;23:195–202.
[60] BioLuminate Inc. 2000. Available from: http://www.bioluminate.com/description.html.
[61] Breckon WR, Pidcock MK. Data errors and reconstruction algorithms in electrical impedance tomography. Clin Phys Physiol Meas 1988;9:A105–A9.

[62] Brown BH, Barber DC. Possibilities and problems of real-time imaging of tissue resistivity. Clin Phys Physiol Meas 1988;9:A121–A5.
[63] Hua P, Woo EJ, Webster JG, Tompkins WJ. Finite element modeling of electrode-skin contact impedance in electrical impedance tomography. IEEE Trans Biomed Eng 1993;40:29–34.
[64] Hua P, Woo EJ, Webster JG, Tompkins WJ. Using compound electrodes in electrical impedance tomography. IEEE Trans Biomed Eng 1993;40:29–34.
[65] Li J. A method of reducing the error caused by boundary shape and electrode positions in electrical impedance tomography. Physiol Meas 1994;15:A169–A74.
[66] Boone KG, Holder DS. Effect of skin impedance on image quality and variability in electrical impedance tomography: a model study. Med Biol Eng Comput 1996;34:351–4.
[67] Kolehmainen V, Vauhkonen M, Karjalainen PA, Kaipio JP. Assessment of errors in static electric impedance tomography with adjacent and trigonometric current patterns. Physiol Meas 1997;18:289–303.
[68] Blott BH, Daniell GJ, Meeson S. Electrical impedance tomography with compensation for electrode positioning variations. Phys Med Biol 1998;43:1731–9.
[69] McAdams ET, McLaughlin JA, Anderson JM. Multi-electrode systems for electrical impedance tomography. Physiol Meas 1994;15:A101–A6.
[70] Jossinet J. A hardware design for imaging the electrical impedance of the breast. Clin Phys Physiol Meas 1988;9:A25–A8.
[71] Holder DS. Design and electrical characteristics of an electrode array for electrical impedance tomography of the female breast. Innov Technol Biol Med 1995;16(S.I. 2):143–50.
[72] Cornish BH, Jacobs A, Thomas BJ, Ward LC. Optimizing electrode sites for segmental bioimpedance measurements. Physiol Meas 1999;20(3):241–50.
[73] Smith DG, Potter SR, Lee BR, Ko HW, Drummond WR, Telford JK et al. In vivo measurement of tumor conductiveness with the magnetic bioimpedance method. IEEE Trans Biomed Eng 2000;47:1403–5.
[74] Jossinet J, Lavandier B, Cathignol D. Impedance modulation by pulsed ultrasound. Ann N Y Acad Sci 1999;873:396–407.